AGU PUBLICATIONS

Paleoceanography

RESEARCH ARTICLE
10.1002/2012PA002417

Key Points:
- Timing of rainy season changed during the middle to late Holocene over northern SCS
- Variation patterns of rainy season agreed with magnetic susceptibility records
- Shift of rainy season may be associated with ITCZ and atmospheric circulation

Supporting Information:
- Readme
- Supplementary Figures S1–S3

Correspondence to:
G. Wei,
gjwei@gig.ac.cn

Citation:
Deng, W., G. Wei, K. Yu, and J.-x. Zhao (2014), Variations in the timing of the rainy season in the northern South China Sea during the middle to late Holocene, *Paleoceanography*, *29*, 115–125, doi:10.1002/2012PA002417.

Received 15 OCT 2012
Accepted 10 JAN 2014
Accepted article online 15 JAN 2014
Published online 18 FEB 2014

Variations in the timing of the rainy season in the northern South China Sea during the middle to late Holocene

Wenfeng Deng[1], Gangjian Wei[1], Kefu Yu[2], and Jian-xin Zhao[3]

[1]State Key Laboratory of Isotope Geochemistry, Guangzhou Institute of Geochemistry, Chinese Academy of Sciences, Guangzhou, China, [2]Key Laboratory of Marginal Sea Geology, South China Sea Institute of Oceanology, Chinese Academy of Sciences, Guangzhou, China, [3]Radiogenic Isotope Laboratory, Centre for Microscopy and Microanalysis, University of Queensland, Brisbane, Queensland, Australia

Abstract The amount and timing of precipitation in East Asia are important aspects of the East Asian monsoon. Many paleoclimate records that act as proxies for wet or dry climatic conditions have been linked to changes in precipitation amounts and are thus used to indicate changes in the East Asian monsoon system. However, few studies have examined changes in the timing of the rainy season. Here, we consider the timing of the seasonal precipitation cycle during the middle to late Holocene, using records derived from coupled high-resolution Sr/Ca and $\delta^{18}O$ records preserved in *Porites* corals from the northern South China Sea. These records indicate that the timing of the rainy season in this region changed during the middle to late Holocene. The present-day rainy season generally occurs over the summer and autumn (June–October), which has also been recorded in *Porites* coral, whereas the rainy season at around 1500 and 6800 years B.P. occurred through the autumn and winter (August–December), and the rainy season at around 2540 and 5000 years B.P. occurred in the winter and spring (January–April or December–March). During the period around 5900 years B.P., the seasonal distribution of precipitation varied from year to year. These shifts in the timing of the rainy season require changes in temperature and humidity patterns and appear to agree with changes in the magnetic susceptibility of lake sediments in this region, which may reflect movements of the Intertropical Convergence Zone location and changes in atmospheric circulation during the middle to late Holocene.

1. Introduction

The climate of East Asia is dominated by the monsoon [*An*, 2000]. Generally, winds blow toward land in summer, bringing abundant rainfall, whereas they blow toward the sea in winter, resulting in a relatively dry climate. As a result, most of the precipitation occurs during the warm seasons [*Wang et al*., 2005], with almost synchronous seasonal variations in temperature and precipitation. Natural ecosystems and human activities in this region appear to have adapted to this seasonal pattern; e.g., the period of warm and rainy conditions during late spring and summer in South China favors the growth of rice [*Timsina and Connor*, 2001].

Global trends in climate change are accompanied by uncertainties [*Folland et al*., 2001; *Reilly et al*., 2001; *Karl and Trenberth*, 2003; *Webster et al*., 2003; *Hegerl et al*., 2007]. If climate change modifies the synchronous variations of temperature and precipitation, the seasonal distribution of precipitation may change, potentially leading to prolonged drought in summer or heavy snow and rainfall in winter. A study of the evolution of the hydrologic system suggests that the seasonal balance of precipitation over the inland Pacific Northwest has shifted from 10% to 50% falling in the winter and 50% to 90% in summer during the last glacial period, to the current situation of around 75% falling in the winter and 25% in summer [*Takeuchi*, 2007]. A change in the rainy season would have a significant impact on ecosystems and disastrous consequences for social and economic development. For example, persistent and heavy rain and snow in South China lasted for more than a month during the winter of 2008 [*Ding et al*., 2009] and resulted in at least 129 deaths, U.S. $15.4 billion of direct economic losses, and disruption to the lives of more than 400 million people, as well as affecting industrial and agricultural production [*National Climate Center*, 2008].

Little is known about long-term changes in the timing of the rainy season in East Asia, including the mechanism of change, the factors that disturb the synchronicity of precipitation and temperature, and future

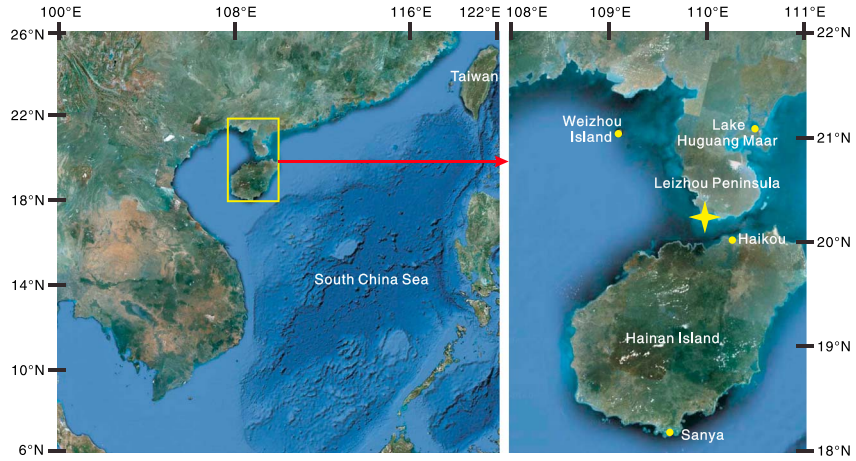

Figure 1. Satellite image of the Leizhou Peninsula. The star indicates the sample location. Instrumental SST is monitored at Haikou and SSS at Weizhou Island. The coral-based rainy season study site of *Deng et al.* [2009] was at Sanya.

patterns. These uncertainties may be addressed by examining historical records of changes in the timing of the rainy season. However, instrumental observations in this region only extend over the past several decades, which is insufficient to examine temporal variations in the timing of the rainy season. To develop a better understanding of such changes over longer timescales, it is necessary to extend the historical records using proxies [*Mann*, 2002; *Jansen et al.*, 2007; *Jones et al.*, 2009]. In this regard, massive corals provide the most reliable archives, as they contain clear annual bands and have high growth rates, thereby providing a detailed record of seasonal variations in paleoclimate [*Gagan et al.*, 2000; *Grottoli*, 2001; *Cole*, 2003; *Felis and Pätzold*, 2003; *Lough*, 2010], including changes in the seasonal distribution of precipitation [*Deng et al.*, 2009]. Sr/Ca ratios in coral skeletons have long been used to reconstruct changes in sea surface temperature (SST) [*Smith et al.*, 1979; *Beck et al.*, 1992; *McCulloch et al.*, 1999] and $\delta^{18}O$ values in coral reflect SST and $\delta^{18}O$ in ambient seawater [*Swart and Coleman*, 1980; *Dunbar and Wellington*, 1981]. Residual $\delta^{18}O$ (i.e., $\Delta\delta^{18}O$), which is calculated by subtracting the contribution of temperature from coral $\delta^{18}O$, can be used as a tracer of temporal changes in seawater $\delta^{18}O$ ($\delta^{18}O_{sw}$) [*McCulloch et al.*, 1994; *Gagan et al.*, 1998, 2000; *Corrège*, 2006]. In areas where freshwater input is a key contributing factor to variations in seawater $\delta^{18}O$, $\delta^{18}O_{sw}$ can trace temporal changes in precipitation [*McCulloch et al.*, 1994; *Shen et al.*, 2005]. As $\delta^{18}O$ in freshwater is generally more negative than that in seawater, minimum $\delta^{18}O_{sw}$ values typically indicate the maximum input of freshwater, and thus the occurrence of peak precipitation, i.e., the rainy season. Assuming that SST shows seasonal changes, the phase offset between peaks in $\delta^{18}O_{sw}$ and SST may also provide information on seasonal changes in precipitation [*Shen et al.*, 2005] and change in the timing of the rainy season could be estimated from the phase angles of the cross-spectral analysis of $\delta^{18}O_{sw}$ and SST records [*Deng et al.*, 2009].

An ideal site for the investigation of changes in the timing of the rainy season is the coastal region of South China, next to the northern South China Sea (SCS), where seasonal variations in precipitation are significant, with over 80% of the annual precipitation occurring between May and October. The heavy precipitation during the rainy season causes the peak river runoff to the coastal region, strongly influencing the isotopic and elemental records preserved in corals [*Wei et al.*, 2000]. Our recent study showed that seasonal change in $\delta^{18}O_{sw}$ is a reliable proxy for the rainy season and that the timing of the rainy season on Hainan Island during the mid-Holocene differed to that of the present-day rainy season [*Deng et al.*, 2009].

Here we revisit the Sr/Ca-SST and $\delta^{18}O$ records of the middle to late Holocene corals from the Leizhou Peninsula (20°13–17′N, 109°54–58′E), northern SCS (Figure 1), of *Yu et al.* [2005]. The $\delta^{18}O_{sw}$ values obtained from these corals are reexamined and the time offsets between the $\delta^{18}O_{sw}$ and SST records estimated using cross-spectral analysis. The time offsets indicate temporal change in the timing of the rainy season in this region from the middle to late Holocene. In turn, this provides information on changes in the timing of the rainy season in the northern SCS and enables a better understanding of the evolution of the East Asian monsoon.

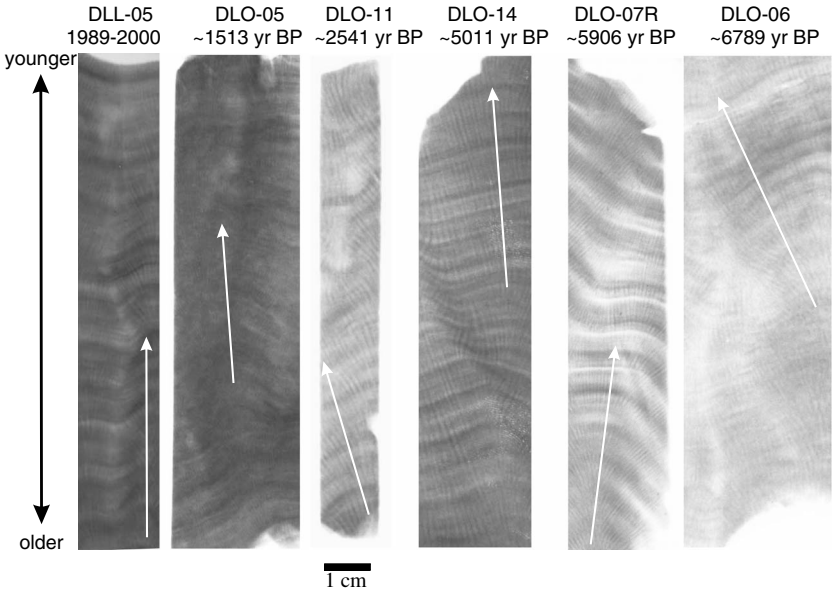

Figure 2. X-radiographs of one modern and five *Porites lutea* fossil corals collected from the Leizhou Peninsula. Arrows indicate the direction of the maximum growth axes.

2. Materials and Methods

We analyzed one modern and five fossil *Porites lutea* corals collected from the low-tidal emerged reef flat on the Leizhou Peninsula, northern SCS (Figure 1). The ages of the five fossil corals ranged from A.D. 487 to 4789 B.C., and their growth periods were approximately 10 years [*Yu et al*., 2005]. The total length of these samples would probably not allow a distinction between the older and younger ages measured by the ^{238}U-^{234}U-^{230}Th method with its associated dating uncertainty of decades. However, the well-preserved fossil corals were in situ growth and without any transitional forms (supporting information Figure S1), so their top (youngest part) and bottom (oldest part) could be clearly identified (supporting information Figures S2 and S3), enabling a definite sampling direction from the youngest to the oldest for all six corals. In addition, the direction of the maximum growth axes of these corals can be clearly identified in the X-radiographs of the coral slices (Figure 2), which provides further guidance for the sampling direction.

The growth chronologies of the corals were constructed using Sr/Ca ratios, assuming that each Sr/Ca cycle represents 1 year, and by cross-validating this approach with visual observations from the X-radiographs. Sr/Ca maxima were assigned to the beginning (January) of each year, which is generally the coldest time in this region and used as time control points. Monthly time resolution was obtained by linear interpolation (for an annual cycle with <12 data points) or by averaging the nearest neighbor data (for an annual cycle with >12 data points). The top and bottom of the coral cores were assigned the youngest and the oldest ages, respectively.

SSTs derived from the Sr/Ca ratios, and the δ^{18}O and $\Delta\delta^{18}$O values of these corals, have previously been analyzed to assess temporal changes in the strength of the summer monsoon during the middle to late Holocene [*Yu et al*., 2005]; however, variations in the timing of the rainy season have yet to be explored. Values of $\delta^{18}O_{sw}$ ($\Delta\delta^{18}$O) were calculated by the method of *Gagan et al*. [1998]; i.e.,

$$\delta^{18}O_{sw}\left(\Delta\delta^{18}O\right) = d\delta^{18}O/dT \times \left[T_{\delta 18O} - T_{Sr/Ca}\right]$$

where $d\delta^{18}O/dT$ is the slope of the empirical δ^{18}O-SST relationship and $T_{\delta 18O}$ and $T_{Sr/Ca}$ are the apparent SSTs calculated from the δ^{18}O and Sr/Ca ratios, respectively. The slopes for $d\delta^{18}O/dT$ and $d(Sr/Ca)/dT$ are -0.017‰/°C and -0.0424 mmol/mol/°C, respectively [*Yu et al*., 2005]. This study focuses on the temporal relationship between the variation in SST and $\delta^{18}O_{sw}$, and the influence of seawater δ^{18}O variation on the coral δ^{18}O-SST relationship was not considered. Some studies argue that this may result in large errors in $\delta^{18}O_{sw}$ and makes it problematic to use $\delta^{18}O_{sw}$ to estimate changes in seawater δ^{18}O [*Ren et al*., 2003; *Cahyarini*

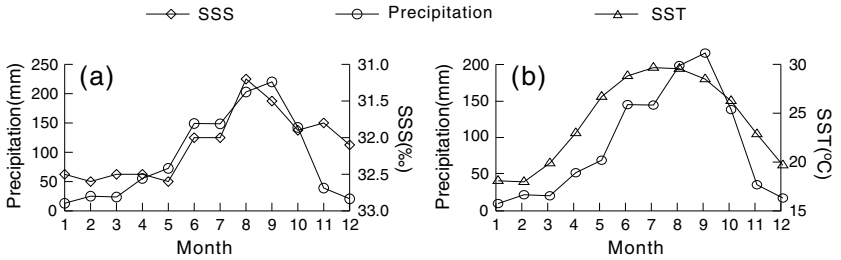

Figure 3. Time series of mean monthly precipitation, SSS, and SST. Precipitation data are from the meteorological observatory at the Xuwen Salt Factory (1.5 km from the sampling site) for the period A.D. 1975–2000. SSS data are from the ocean observatory on Weizhou Island (110 km from the sampling site) for the period A.D. 1960–1994. SST data are from Haikou Ocean Observatory (47 km from the sampling site) for the period A.D. 1960–2000.

et al., 2008]. Several new methods have been proposed to calculate $\delta^{18}O_{sw}$, which may partially reduce the possible errors related to the calibration of coral $\delta^{18}O$ with SST [*Ren et al*., 2003; *Cahyarini et al*., 2008]. However, *Huppert and Solow* [2004] demonstrated that the method of *Ren et al*. [2003] is essentially the same as that of *Gagan et al*. [1998]. And, while the $\delta^{18}O_{sw}$ values obtained by the methods of *Cahyarini et al*. [2008] and *Gagan et al*. [1998] have different absolute values, they have the same pattern of variation and a good positive correlation [*Deng et al*., 2009]. This study is mainly concerned with identifying patterns of variation in the $\delta^{18}O_{sw}$ record to determine the timing of precipitation rather than to quantitatively reconstruct past seawater $\delta^{18}O$. Values of $\delta^{18}O_{sw}$ ($\Delta\delta^{18}O$) calculated using the method of *Gagan et al*. [1998] can reliably indicate changing patterns of seawater $\delta^{18}O$, and hence changes in the pattern of precipitation over the northern SCS, as has been demonstrated by *Deng et al*. [2009].

Changes in the timing of the rainy season can be estimated from the temporal offset between $\delta^{18}O_{sw}$ and SST records. Recent observations (A.D. 1975–2000) indicate that more than 80% of the annual precipitation on the Leizhou Peninsula falls between June and October (Figure 3). This peak in precipitation is associated with a marked decrease in the $\delta^{18}O$ value of surface seawater around coastal coral reefs, corresponding to strongly negative $\delta^{18}O_{sw}$ peaks in the coral skeletons [*Yu et al*., 2005]. Assuming that temperature change correlates with changes in the seasons (i.e., maximum temperatures indicate midsummer, while minimum temperatures indicate midwinter), the time offset between negative $\delta^{18}O_{sw}$ peaks and maximum SSTs may indicate the season with the greatest precipitation, i.e., the rainy season. Such time offsets can be estimated quantitatively using cross-spectral analysis, which has been used in paleoclimate studies to identify phase relationships between two harmonic time series [*Schulz and Stattegger*, 1997]. This method has successfully been established and used to estimate changes in the timing of the rainy season at around 6500 years B.P. on Hainan Island, northern SCS [*Deng et al*., 2009]. The feasibility of this method is further demonstrated in the present study.

3. Results

The Sr/Ca-SST and $\delta^{18}O_{sw}$ values from the six corals are shown in Figure 4. Both time series show clear annual cycles but with variable time offsets between the two data sets. The negative $\delta^{18}O_{sw}$ peaks generally lag behind the maximum summer SSTs in the records from A.D. 1989 to 2000, A.D. 487 ± 22, and 4789 ± 43 B.C. In contrast, the negative $\delta^{18}O_{sw}$ peaks generally lead the maximum summer SSTs in the records from 541 ± 24 BC and 3011 ± 54 B.C. At 3906 ± 28 B.C., the temporal relationship between the $\delta^{18}O_{sw}$ and SST is complex, with variable leads and lags between the negative $\delta^{18}O_{sw}$ peaks and the maximum SSTs.

Figure 5 shows the mean monthly variations in Sr/Ca-SST and $\delta^{18}O_{sw}$, calculated by averaging the data for each month. The leads and lags between the negative $\delta^{18}O_{sw}$ peaks and the maximum SSTs are similar to those in Figure 4.

The time offset between the records of $\delta^{18}O_{sw}$ and SST was estimated using the phase angles of the cross-spectral analysis between the two records [*Deng et al*., 2009], using the software SPECTRUM [*Schulz and Stattegger*, 1997]. These phase angles, and the corresponding time offsets, are summarized in Table 1. The results show that the timing of the rainy season changed significantly during the middle to late Holocene in this region, from around 4.0 months ahead of the present-day situation to around 4.5 months behind, as described in more detail below.

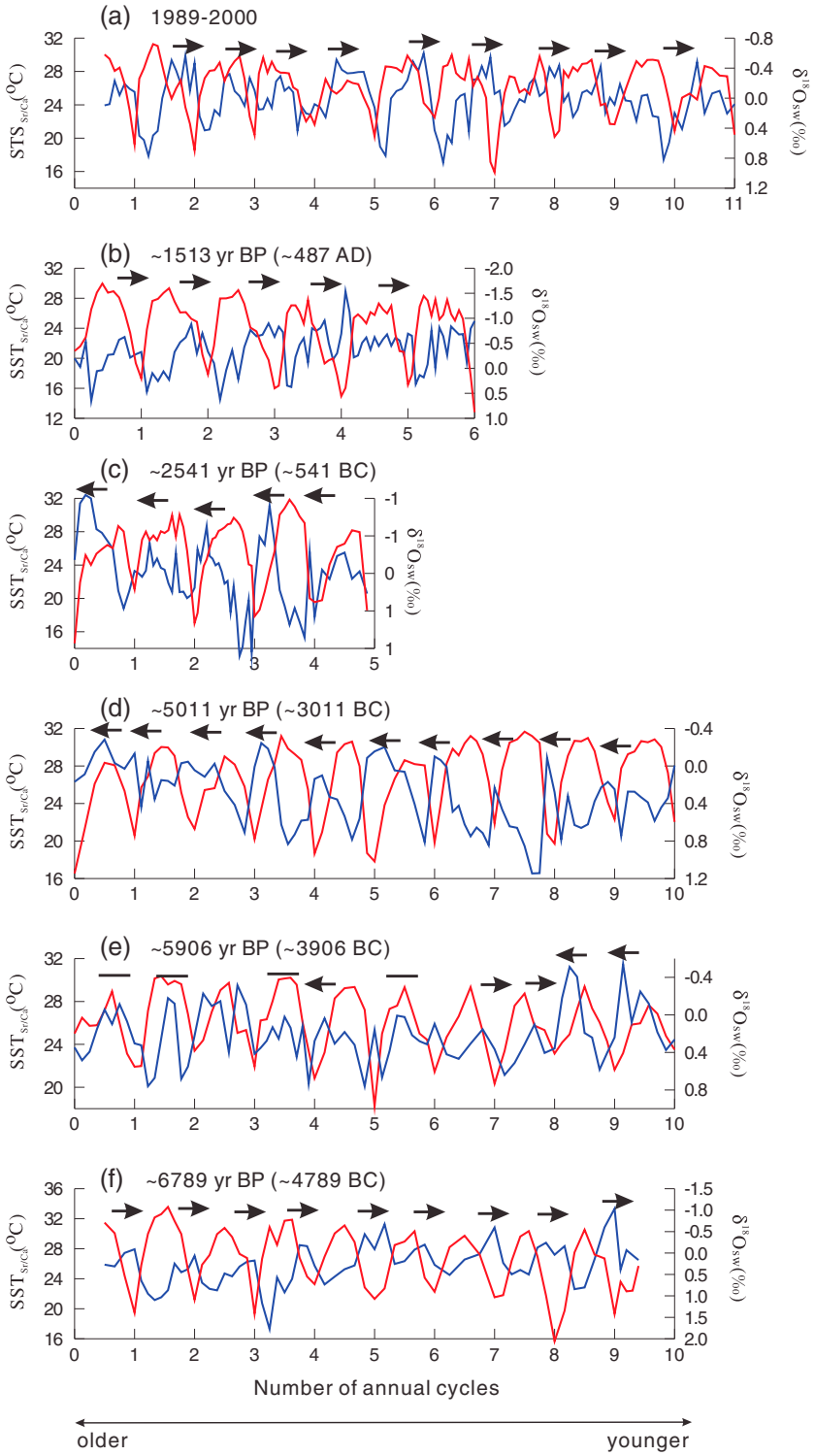

Figure 4. Time series of $\delta^{18}O_{sw}$ and Sr/Ca-SST values reconstructed from middle to late Holocene and modern corals. See text for discussion. The red lines are Sr/Ca-SST records; blue lines are $\delta^{18}O_{sw}$ records. Right-facing arrows indicate that $\delta^{18}O_{sw}$ follows Sr/Ca-SST and vice versa. Lines without arrowheads indicate that $\delta^{18}O_{sw}$ and Sr/Ca-SST are synchronous.

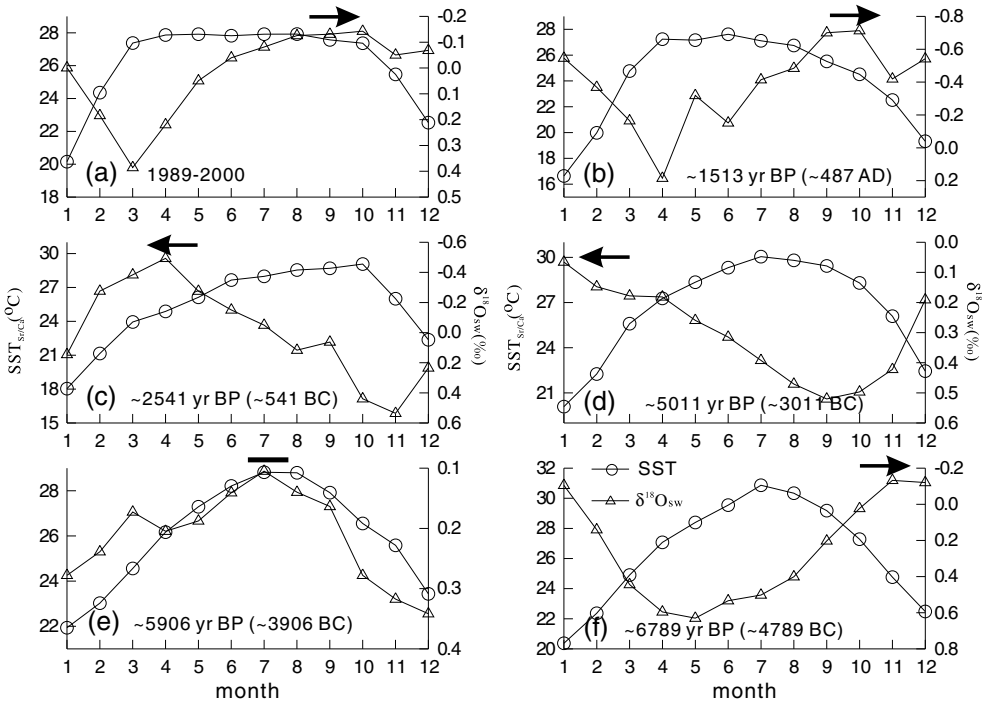

Figure 5. Time series of mean monthly $\delta^{18}O_{sw}$ and Sr/Ca-SST reconstructed from middle to late Holocene and modern corals. See text for discussion. Right-facing arrows indicate that $\delta^{18}O_{sw}$ follows Sr/Ca-SST and vice versa. Lines without arrowheads indicate that $\delta^{18}O_{sw}$ and Sr/Ca-SST are synchronous.

3.1. Circa 1513 Years B.P. (A.D. 487)

The temporal relationship between $\delta^{18}O_{sw}$ and SST in the coral from around 1513 years B.P. is similar to that in modern coral, with negative $\delta^{18}O_{sw}$ peaks significantly lagging behind the maximum SST (Figures 4b and 5b). The time offset between the two records is -4.0 ± 0.7 months; thus, the rainy season during this period may have occurred approximately $4.0 - 2.5 = 1.5$ months later than in the present day (i.e., from August to December).

3.2. Circa 2541 Years B.P. (541 B.C.)

In contrast to the modern coral, the negative $\delta^{18}O_{sw}$ peaks in the coral from around 2541 years B.P. precede the SST maxima (Figures 4c and 5c) by 3.5 ± 0.3 months. Thus, the rainy season during this period was $2.5 + 3.5 = 6.0$ months ahead of the modern timing and occurred between January and April.

3.3. Circa 5011 Years B.P. (3011 B.C.)

Similar to the coral from around 2541 years B.P., the negative $\delta^{18}O_{sw}$ peaks in the coral from around 5011 years B.P. lead the SST maxima (Figures 4d and 5d) by 4.5 ± 0.1 months (Table 1). Therefore, the rainy season during this period was approximately $2.5 + 4.5 = 7$ months ahead of the June–October period of the modern day (i.e., during winter, from December to March).

Table 1. Time Offset Between Sr/Ca-SST and $\delta^{18}O_{sw}$ Estimated by Cross-Spectral Analysis

Period	Phase Angle[a] (Deg)	Time Offset (Month)	Instrumental or Inferred Rainy Season
1989–2001	-80 ± 10	-2.5 ± 0.3	Jun to Oct
Circa 1513 years B.P. (487 A.D.)	-121 ± 20	-4.0 ± 0.7	Aug to Dec
Circa 2541 years B.P. (541 B.C.)	106 ± 10	3.5 ± 0.3	Jan to Apr
Circa 5011 years B.P. (3011 B.C.)	140 ± 3	4.5 ± 0.1	Dec to next Mar
Circa 5906 years BP (3906 B.C.)	0	0	Irregular
Circa 6789 years B.P. (4789 BC)	-129 ± 15	-4.3 ± 0.5	Aug to Dec

[a]Negative phase angles indicate that $\delta^{18}O_{sw}$ lags precipitation and vice versa.

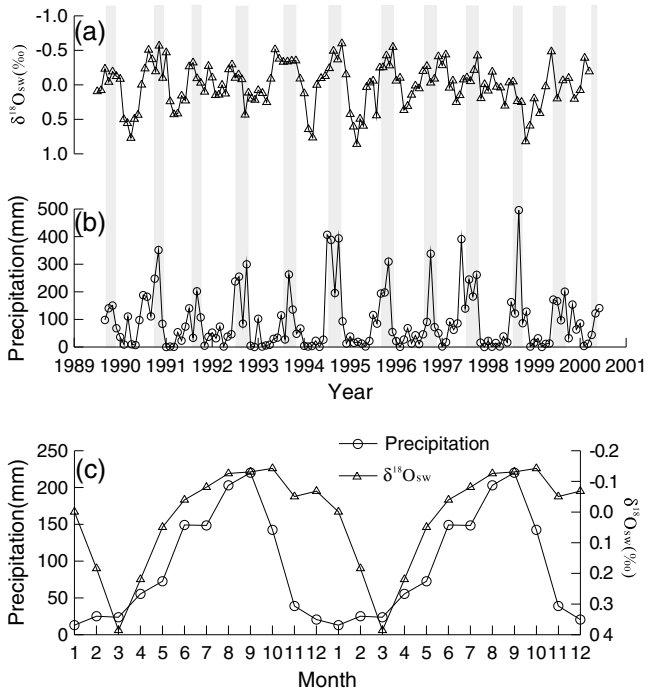

Figure 6. Time series of modern day coral $\delta^{18}O_{sw}$ and precipitation. (a) Modern coral $\delta^{18}O_{sw}$ record. (b) Modern precipitation record. (c) Monthly coral $\delta^{18}O_{sw}$ and precipitation records. Two identical annual cycles of mean monthly variations from the two records are shown to highlight the synchronous variations of coral $\delta^{18}O_{sw}$ and precipitation. The precipitation data are the same as those in Figure 3.

3.4. Circa 5906 Years B.P. (3906 B.C.)

The coral from around 5906 years B.P. shows complicated time offsets between the negative $\delta^{18}O_{sw}$ peaks and SST maxima (Figures 4e and 5e). Both leads and lags are observed, and in some years the negative $\delta^{18}O_{sw}$ peaks are synchronous with the SST maxima. As a result, cross-spectral analysis between the two records did not yield a consistent value for the time offsets between them (Table 1), suggesting that the timing of the rainy season varied from year to year during this period.

3.5. Circa 6789 Years B.P. (4789 B.C.)

The negative $\delta^{18}O_{sw}$ peaks of the coral from around 6789 years B.P. lag the SST maxima (Figures 4f and 5f) by -4.3 ± 0.5 months (Table 1), which is similar to the lag recorded in the modern coral. Thus, the rainy season at around 6789 years B.P. was $4.3 - 2.5 = 1.8$ months later than that of the modern day (i.e., from August to December).

In summary, the timing of the rainy season on the Leizhou Peninsula was variable during the middle to late Holocene. In contrast to the summer–autumn rainy season (June–October) of the modern day, the rainy season occurred between August and December at around 1500 and 6800 years B.P., from December to March at around 5000 years B.P., and from January to April at around 2500 years B.P. Around 5900 years B.P., there was no consistent trend in the timing of precipitation, which varied from year to year.

4. Discussion

4.1. Values of $\delta^{18}O_{sw}$ as a Proxy for the Timing of the Rainy Season

Concentrated precipitation during the rainy season is generally associated with peak river runoff into coastal reefs, resulting in low sea surface salinity (SSS) and a negative $\delta^{18}O_{sw}$ peak being preserved in coral skeletons. These factors are therefore a reliable proxy for the timing of the rainy season, and this relationship has been well documented on southern Hainan Island and used to reconstruct the record of the rainy season in this region [*Deng et al.*, 2009].

On the Leizhou Peninsula, the rainy season generally occurs between June and October, with peak precipitation falling in August and September (Figure 3) [*Yu et al.*, 2005]. Consequently, the SSS near the coral reefs shows a minimum in August and September (Figure 3a). Temporal variations in the modern $\delta^{18}O_{sw}$ record are in agreement with the instrumental precipitation record, with negative $\delta^{18}O_{sw}$ peaks generally corresponding to precipitation maxima (Figures 6a and 6b), except in 1997 and 1998, possibly due to the effects of the El Niño–La Niña cycle on the SST and rainfall in the northern SCS at that time [*Ciesielski and Johnson*, 2006]. Moreover, variations in the mean monthly $\delta^{18}O_{sw}$ values of the modern coral are generally in step with those of precipitation (Figure 6c). To highlight this synchronous variation more clearly, two identical annual cycles of mean monthly variations in the two records are presented. The similarity of temporal variations in precipitation, SSS, and coral $\delta^{18}O_{sw}$ supports the proposal that the coral $\delta^{18}O_{sw}$ record is a good proxy for temporal change in the timing of the rainy season in this region.

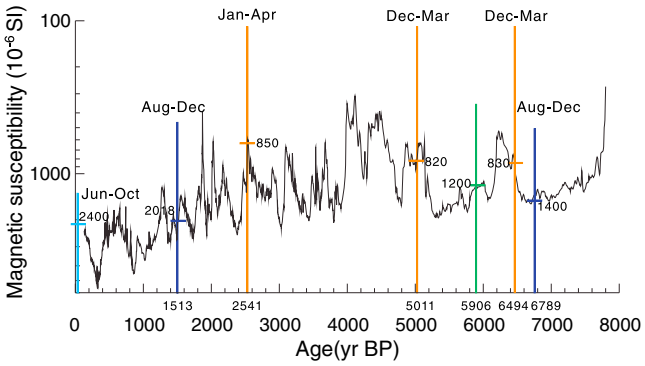

Figure 7. Inferred timing of the rainy season in the middle to late Holocene and comparison with the magnetic susceptibility of sediments from Lake Huguang Maar. See text for discussion. Vertical lines and corresponding months indicate the timing of the rainy season. Horizontal bars and corresponding numbers indicate magnetic susceptibility values. Magnetic susceptibility data are from *Yancheva et al.* [2007].

In terms of coral paleoclimate records, seasonal changes can be represented by monthly SST cycles derived from Sr/Ca ratios. Using this approach, the occurrence of peak precipitation or the rainy season can be inferred from the time offsets between $\delta^{18}O_{sw}$ and Sr/Ca-SST trends [*Deng et al.*, 2009]. Negative $\delta^{18}O_{sw}$ peaks generally lag behind Sr/Ca-SST maxima in modern coral (Figures 4a and 5a) by 2.5 ± 0.3 months (Table 1), as estimated by cross-spectral analysis. This finding agrees with the time offsets between SST and precipitation during the period A.D. 1960–2000. As shown in Figure 3b, the mean monthly precipitation maximum occurs in September on the Leizhou Peninsula, while the mean monthly SST maximum occurs in July. Thus, the time offset between $\delta^{18}O_{sw}$ and SST in coral records is equal to that between observed precipitation and SST (Figure 3b). Again, this finding supports the reliability of coral $\delta^{18}O_{sw}$ as a proxy for the seasonal distribution of precipitation and shows the feasibility of using the time offsets between $\delta^{18}O_{sw}$ and SST records in corals to reconstruct the timing of the rainy season in this region.

4.2. Possible Evidence for a Change in the Timing of the Rainy Season Over the Northern SCS

Previous studies have reported temporal changes in the timing of the rainy season over the northern SCS. Even so, historical studies of rainy season trends remain scarce. A coral record from Nanwan Bay, southern Taiwan, showed a relatively early occurrence of the rainy season during some years around 6730 years B.P. [*Shen et al.*, 2005]. Our latest study at Sanya Bay, southern Hainan Island, which focused on a period of more than 30 years around 6494 years B.P., indicated that the rainy season started in December–January and continued until early spring [*Deng et al.*, 2009]. Pollen records also suggested that thermal and humidity conditions may have become decoupled around 6000–7000 years B.P. in central Taiwan [*Liew et al.*, 2006]. These results, together with those of the present study, indicate that the timing of the rainy season over the northern SCS was variable during the middle to late Holocene.

The changes in the rainy season appear to correspond to other paleoclimate records from the northern SCS. Near-annual time-resolved magnetic susceptibility records from sediments in Lake Huguang Maar (located 120 km from the coral reefs off the Leizhou Peninsula) indicate temporal variations in the monsoon climate [*Yancheva et al.*, 2007]. It is interesting to note that the winter–spring rainy seasons at around 2541 and 5011 years B.P. in this region, and at around 6494 years B.P. on southern Hainan Island, generally coincide with periods of low magnetic susceptibility (600–800 × 10^{-6} Système Internationale, SI). In contrast, the autumn–winter rainy seasons, at around 1513 and 6789 years B.P., coincide with phases of high magnetic susceptibility (1400–2100 × 10^{-6} SI) (Figure 7), and this is also the case for the present-day summer–autumn rainy season (approximately 2400 × 10^{-6} SI). In addition, the period around 5906 years B.P., which shows no consistent seasonal distribution of precipitation, yields a moderate susceptibility value (approximately 1200 × 10^{-6} SI) (Figure 7).

Such variations in magnetic susceptibility have previously been related to changes in the strength of the winter monsoon, as an enhanced winter monsoon could deliver larger amounts of wind-blown magnetic material from inland China [*Yancheva et al.*, 2007]. However, geochemical studies of the sediments in Lake Huguang Maar indicate that the local products of chemical weathering dominate, with a negligible contribution from aeolian minerals derived from inland China [*Zhou et al.*, 2007]. Thus, variations in magnetic susceptibility mainly indicate changes in the local climate and environment rather than the strength of the winter monsoon. Although magnetic susceptibility is controlled mainly by the amount of magnetic minerals in the sediment, it is also influenced by the grain size of sediments, the species of Fe-bearing minerals, and redox conditions, which are in turn affected by the local climate and other environmental factors.

The warm and humid climate in South China gives rise to high rates of chemical weathering [*Ma et al*., 2007]. Such weathering tends to concentrate Fe-bearing and other magnetic minerals in the weathering products [*Ma et al*., 2007], resulting in the enhanced magnetic susceptibility of soils and sediments [*Yancheva et al*., 2007]. The high temperatures and humidity of the current summer–autumn rainy season of South China causes intensive chemical weathering. Consequently, sediments from the upper section of the core from Lake Huguang Maar yield high values of magnetic susceptibility (approximately 2400 SI; Figure 7). The occurrence of a winter–spring rainy season at around 2500, 5000, and 6500 years B.P. may have been associated with a relatively dry warm season (summer–autumn), which would not favor intense chemical weathering. Consequently, the sediments of this age in Lake Huguang Maar yield low values of magnetic susceptibility (820–850 SI; Figure 7). For the periods around 1500 and 6800 years B.P., when the rainy season occurred during the late autumn to early winter, the relative timing of the periods of high temperature and humidity was moderately favorable to chemical weathering (i.e., less favorable than the present situation but more favorable than the conditions at 2500, 5000, and 6500 years B.P.), yielding intermediate values of magnetic susceptibility (Figure 7). For the period around 5900 years B.P., when the timing of the rainy season was variable, the magnetic susceptibility was approximately 1200 SI, higher than that for the period with a winter–spring rainy season but lower than that from other periods (Figure 7). The agreement between the timing of the rainy season, as derived from our coral records, and the magnetic susceptibility of sediments at Lake Huguang Maar is consistent with our hypothesis of a link between the coral and sediment records and supports the reliability of reconstructing variations in the timing of the rainy season from coral records.

4.3. Possible Mechanisms for a Change in the Timing of the Rainy Season Over the Northern SCS

Recent paleoclimate studies suggest that the annual mean position of the Intertropical Convergence Zone (ITCZ) has changed in the past due to changes in the strength of the summer monsoon [*Fleitmann et al*., 2007; *Yancheva et al*., 2007]. The migration of the ITCZ may influence the spatial and temporal distribution of peak precipitation [*Fleitmann et al*., 2007]. A coral-based reconstruction of ITCZ variability over Central America indicated that the zone of maximum rainfall in the eastern Pacific has expanded northward during each Northern Hemisphere summer since 1707 [*Linsley et al*., 1994]. Another recent study of coral records also suggests that a northward shift of the ITCZ could have led to less precipitation over the SCS but increased continental precipitation for inland Asia during the mid-Holocene [*Yokoyama et al*., 2011]. Therefore, it is very likely that a change in the strength of the Asian Monsoon, and a shift in the position of ITCZ, could cause variations in the timing of the rainy season over the northern South China Sea.

No previous study has performed detailed numerical modeling of temporal changes in the timing of the rainy season. Changes in atmospheric circulation may cause a shift in the rainy season over the northern SCS (B. Wang, University of Hawaii, personal communication, 2008). According to numerical modeling of the Asian summer monsoon [*Chou*, 2003], the major rainband during the middle to late Holocene developed to the north of its present-day location, because of the relatively strong summer monsoon that created a dipole pattern in rainfall anomalies (negative in the south and positive in the north). The northern SCS is located in the southern negative region, indicating reduced summer rainfall and maximum rainfall during the autumn and winter (C. Chou, Academia Sinica, personal communication, 2009). The springtime rainy season may be associated with an enhanced springtime frontal system (C. Chou, personal communication, 2009), although this possibility requires further examination.

5. Conclusions

In this paper we have reconstructed changes in the seasonal precipitation cycle over the northern SCS during the middle to late Holocene, based on coupled Sr/Ca and $\delta^{18}O$ records from reef corals. Our results indicate temporal variations in the timing of the rainy season during this period. Unlike the current summer and autumn rainy season (June–October), the rainy season during the middle to late Holocene occurred during the autumn and winter (August–December) around 1513 and 6789 years B.P., but in winter and spring around 5011 years B.P. (December–March) and 2541 years B.P. (January–April). The timing of precipitation showed no consistent pattern during the period around 5906 years B.P. Migration of the position of the ITCZ may have caused a shift in the rainy season timing during the middle to late Holocene. A relatively strong summer monsoon in Asia during the middle to late Holocene drove the ITCZ northward of its present location, along with the location of the main rainband, resulting in negative rainfall anomalies during the summer

for the northern SCS, and a rainfall peak in autumn–winter. A springtime rainy season may be triggered by an enhanced springtime frontal system.

Acknowledgments
The authors would like to thank the Editor Christopher Charles and two anonymous reviewers for their helpful comments and constructive suggestions. Wenfeng Deng offers his special thanks to Chia Chou of Research Center for Environmental Changes, Academia Sinica, and Bin Wang of Department of Meteorology and International Pacific Research Center, the University of Hawaii, for their generous help on the explanation to the shift of rainy season. Thanks also go to Qingsong Liu of Institute of Geology and Geophysics, Chinese Academy of Sciences, for his explanation to some issues on magnetic susceptibility and to Aaron Stallard for improving the English of the manuscript. This work was financed by the National Basic Research Program of China (2013CB956100) and the National Natural Sciences Foundation of China (40902050, 41076025, 40830852, and 41173004). This is contribution IS-1809 from GIGCAS.

References

An, Z. (2000), The history and variability of the East Asian paleomonsoon climate, *Quat. Sci. Rev.*, *19*(1-5), 171–187, doi:10.1016/s0277-3791(99)00060-8.

Beck, J. W., R. L. Edwards, E. Ito, F. W. Taylor, J. Recy, F. Rougerie, P. Joannot, and C. Henin (1992), Sea-surface temperature from coral skeletal strontium/calcium ratios, *Science*, *257*(5070), 644–647.

Cahyarini, S. Y., M. Pfeiffer, O. Timm, W.-C. Dullo, and D. G. Schönberg (2008), Reconstructing seawater δ^{18}O from paired coral δ^{18}O and Sr/Ca ratios: Methods, error analysis and problems, with examples from Tahiti (French Polynesia) and Timor (Indonesia), *Geochim. Cosmochim. Acta*, *72*(12), 2841–2853, doi:10.1016/j.gca.2008.04.005.

Chou, C. (2003), Land–sea heating contrast in an idealized Asian summer monsoon, *Clim. Dyn.*, *21*(1), 11–25, doi:10.1007/s00382-003-0315-7.

Ciesielski, P. E., and R. H. Johnson (2006), Contrasting Characteristics of Convection over the Northern and Southern South China Sea during SCSMEX, *Mon. Weather Rev.*, *134*(4), 1041–1062, doi:10.1175/MWR3113.1.

Cole, J. E. (2003), Holocene coral records: Windows on tropical climate variability, in *Global Change in the Holocene*, edited by A. Mackay et al., pp. 168–184, Arnold, London.

Corrège, T. (2006), Sea surface temperature and salinity reconstruction from coral geochemical tracers, *Paleogeogr. Paleoclimatol. Paleoecol.*, *232*(2-4), 408–428, doi:10.1016/j.palaeo.2005.10.014.

Deng, W. F., G. J. Wei, X. H. Li, K. F. Yu, J. X. Zhao, W. D. Sun, and Y. Liu (2009), Paleoprecipitation record from coral Sr/Ca and δ^{18}O during the mid Holocene in the northern South China Sea, *Holocene*, *19*(6), 811–821, doi:10.1177/0959683609337355.

Ding, Y., X. Jia, Z. Wang, X. Chen, and L. Chen (2009), A contrasting study of freezing disasters in January 2008 and in winter of 1954/1955 in China, *Front. Earth Sci. China*, *3*(2), 129–145, doi:10.1007/s11707-009-0028-2.

Dunbar, R. B., and G. M. Wellington (1981), Stable isotopes in a branching coral monitor seasonal temperature variation, *Nature*, *293*(5832), 453–455.

Felis, T., and J. Pätzold (2003), Climate records from corals, in *Marine Science Frontiers for Europe*, edited by G. Wefer, F. Lamy, and F. Mantoura, pp. 11–27, Springer-Verlag, Berlin Heidelberg New York Tokyo.

Fleitmann, D., et al. (2007), Holocene ITCZ and Indian monsoon dynamics recorded in stalagmites from Oman and Yemen (Socotra), *Quat. Sci. Rev.*, *26*(1-2), 170–188, doi:10.1016/j.quascirev.2006.04.012.

Folland, C. K., et al. (2001), Global temperature change and its uncertainties since 1861, *Geophys. Res. Lett.*, *28*(13), 2621–2624, doi:10.1029/2001GL012877.

Gagan, M. K., L. K. Ayliffe, D. Hopley, J. A. Cali, G. E. Mortimer, J. Chappell, M. T. McCulloch, and M. J. Head (1998), Temperature and surface-ocean water balance of the mid-Holocene tropical western Pacific, *Science*, *279*(5353), 1014–1018, doi:10.1126/science.279.5353.1014.

Gagan, M. K., L. K. Ayliffe, J. W. Beck, J. E. Cole, E. R. M. Druffel, R. B. Dunbar, and D. P. Schrag (2000), New views of tropical paleoclimates from corals, *Quat. Sci. Rev.*, *19*(1-5), 45–64, doi:10.1016/S0277-3791(99)00054-2.

Grottoli, A. G. (2001), Climate: Past climate from corals, in *Encyclopedia of Ocean Sciences*, edited by J. Steele, S. Thorpe, and K. Turekian, pp. 2098–2107, Academic Press, London.

Hegerl, G. C., F. W. Zwiers, P. Braconnot, N. P. Gillett, Y. Luo, J. A. Marengo Orsini, N. Nicholls, J. E. Penner, and P. A. Stott (2007), Understanding and attributing climate change, in *Climate Change 2007: The Physical Science Basis. Contribution of Working Group I to the Fourth Assessment Report of the Intergovernmental Panel on Climate Change*, edited by S. Solomon et al., pp. 663–745, Cambridge Univ. Press, Cambridge, United Kingdom and New York, NY, USA.

Huppert, A., and A. R. Solow (2004), Comment on "Deconvolving the δ^{18}O-seawater component from subseasonal coral δ^{18}O and Sr/Ca at Rarotonga in the southwestern subtropical Pacific for the period 1726 to 1997," by L. Ren, B. K. Linsley, G. M. Wellington, D. P. Schrag, and O Hoegh-Guldberg (2003), *Geochim. Cosmochim. Acta*, *68*(14), 3137–3138, doi:10.1016/j.gca.2003.12.020.

Jansen, E., et al. (2007), Palaeoclimate, in *Climate Change 2007: The Physical Science Basis. Contribution of Working Group I to the Fourth Assessment Report of the Intergovernmental Panel on Climate Change*, edited by S. Solomon et al., pp. 433–497, Cambridge Univ. Press, Cambridge, United Kingdom and New York, NY, USA.

Jones, P. D., et al. (2009), High-resolution palaeoclimatology of the last millennium: A review of current status and future prospects, *Holocene*, *19*(1), 3–49, doi:10.1177/0959683608098952.

Karl, T. R., and K. E. Trenberth (2003), Modern global climate change, *Science*, *302*(5651), 1719–1723, doi:10.1126/science.1090228.

Liew, P. M., C. Y. Lee, and C. M. Kuo (2006), Holocene thermal optimal and climate variability of East Asian monsoon inferred from forest reconstruction of a subalpine pollen sequence, Taiwan, *Earth Planet. Sci. Lett.*, *250*(3-4), 596–605, doi:10.1016/j.epsl.2006.08.002.

Linsley, B. K., R. B. Dunbar, G. M. Wellington, and D. A. Mucciarone (1994), A coral-based reconstruction of Intertropical Convergence Zone variability over central America since 1707, *J. Geophys. Res.*, *99*(C5), 9977–9994, doi:10.1029/94JC00360.

Lough, J. M. (2010), Climate records from corals, *Wiley Interdiscip. Rev.-Clim. Change.*, *1*(3), 318–331, doi:10.1002/wcc.39.

Ma, J. L., G. J. Wei, Y. G. Xu, W. G. Long, and W. D. Sun (2007), Mobilization and re-distribution of major and trace elements during extreme weathering of basalt in Hainan Island, South China, *Geochim. Cosmochim. Acta*, *71*(13), 3223–3237, doi:10.1016/j.gca.2007.03.035.

Mann, M. E. (2002), The value of multiple proxies, *Science*, *297*(5586), 1481–1482, doi:10.1126/science.1074318.

McCulloch, M. T., M. K. Gagan, G. E. Mortimer, A. R. Chivas, and P. J. Isdale (1994), A high-resolution Sr/Ca and δ^{18}O coral record from the Great Barrier Reef, Australia, and the 1982–1983 El Niño, *Geochim. Cosmochim. Acta*, *58*(12), 2747–2754, doi:10.1016/0016-7037(94)90142-2.

McCulloch, M. T., A. W. Tudhope, T. M. Esat, G. E. Mortimer, J. Chappell, B. Pillans, A. R. Chivas, and A. Omura (1999), Coral record of equatorial sea-surface temperatures during the penultimate deglaciation at Huon Peninsula, *Science*, *283*(5399), 202–204, doi:10.1126/science.283.5399.202.

National Climate Center (2008), *Climate Analysis of Low Temperature, Rain and Snow, Freezing Disaster in Early 2008* [in Chinese], Meteorological Press, Beijing, China.

Reilly, J., P. H. Stone, C. E. Forest, M. D. Webster, H. D. Jacoby, and R. G. Prinn (2001), Climate change—Uncertainty and climate change assessments, *Science*, *293*(5529), 430–433, doi:10.1126/science.1062001.

Ren, L., B. K. Linsley, G. M. Wellington, D. P. Schrag, and O. Hoegh-Guldberg (2003), Deconvolving the δ^{18}O-seawater component from subseasonal coral δ^{18}O and Sr/Ca at Rarotonga in the southwestern subtropical Pacific for the period 1726 to 1997, *Geochim. Cosmochim. Acta*, *67*(9), 1609–1621, doi:10.1016/S0016-7037(02)00917-1.

Schulz, M., and K. Stattegger (1997), SPECTRUM: Spectral analysis of unevenly spaced paleoclimatic time series, *Comput. Geosci.*, *23*(9), 929–945, doi:10.1016/S0098-3004(97)00087-3.

Shen, C. C., T. Lee, K. K. Liu, H. H. Hsu, R. L. Edwards, C. H. Wang, M. Y. Lee, Y. G. Chen, H. J. Lee, and H. T. Sun (2005), An evaluation of quantitative reconstruction of past precipitation records using coral skeletal Sr/Ca and $\delta^{18}O$ data, *Earth Planet. Sci. Lett.*, *237*(3-4), 370–386, doi:10.1016/j.epsl.2005.06.042.

Smith, S. V., R. W. Buddemeier, R. C. Redalje, and J. E. Houck (1979), Strontium-calcium thermometry in coral skeletons, *Science*, *204*(4391), 404–407.

Swart, P. K., and M. L. Coleman (1980), Isotopic data for scleractinian corals explain their paleotemperature uncertainties, *Nature*, *283*(5747), 557–559.

Takeuchi, A. (2007), Decoupling the ancient hydrologic system from the modern hydrologic system of Pacific Northwest in the United States: Implications for the evolution of topography, climate, and environment, PhD thesis, Washington State University, Washington, United States.

Timsina, J., and D. J. Connor (2001), Productivity and management of rice-wheat cropping systems: Issues and challenges, *Field Crop. Res.*, *69*(2), 93–132, doi:10.1016/S0378-4290(00)00143-X.

Wang, S. W., R. S. Wu, and X. Q. Yang (2005), Climate change in China, in *Climate Change and Environmental Evolution of China* [in Chinese], edited by D. H. Qin et al., pp. 63-103, Science press, Beijing, China.

Webster, M., et al. (2003), Uncertainty analysis of climate change and policy response, *Clim. Change*, *61*(3), 295–320, doi:10.1023/B:CLIM.0000004564.09961.9f.

Wei, G. J., M. Sun, X. H. Li, and B. F. Nie (2000), Mg/Ca, Sr/Ca and U/Ca ratios of a porites coral from Sanya Bay, Hainan Island, South China Sea and their relationships to sea surface temperature, *Paleogeogr. Paleoclimatol. Paleoecol.*, *162*(1-2), 59–74, doi:10.1016/S0031-0182(00)00105-X.

Yancheva, G., N. R. Nowaczyk, J. Mingram, P. Dulski, G. Schettler, J. F. W. Negendank, J. Q. Liu, D. M. Sigman, L. C. Peterson, and G. H. Haug (2007), Influence of the Intertropical Convergence Zone on the East Asian monsoon, *Nature*, *445*(7123), 74–77, doi:10.1038/nature05431.

Yokoyama, Y., A. Suzuki, F. Siringan, Y. Maeda, A. Abe-Ouchi, R. Ohgaito, H. Kawahata, and H. Matsuzaki (2011), Mid-Holocene palaeoceanography of the northern South China Sea using coupled fossil-modern coral and atmosphere-ocean GCM model, *Geophys. Res. Lett.*, *38*, L00F03, doi:10.1029/2010GL044231.

Yu, K. F., J. X. Zhao, G. J. Wei, X. R. Cheng, and P. X. Wang (2005), Mid-late Holocene monsoon climate retrieved from seasonal Sr/Ca and $\delta^{18}O$ records of *Porites lutea* corals at Leizhou Peninsula, northern coast of South China Sea, *Global Planet. Change*, *47*(2-4), 301–316, doi:10.1016/j.gloplacha.2004.10.018.

Zhou, H. Y., H. Z. Guan, and B. Q. Chi (2007), Record of winter monsoon strength, *Nature*, *450*(7168), E10–E11, doi:10.1038/nature06408.